AIAA JOURNAL
Vol. 30, No. 11, November 1992

Dynamics of Skin-Stringer Panels Using Modified Wave Methods

Donald E. Huntington* and Constantinos S. Lyrintzis†
San Diego State University, San Diego, California 92182

The response of a damped, periodic, simply supported skin-stringer structure is studied by two variants of the decaying wave method. The proposed method is based on a combination of a wave propagation method with transfer matrices. One variant of the decaying wave method is based on an exact solution transfer matrix; the other is based on a finite element formulation. It is shown that both variants give response curves that compare very well with previous results for the undamped structure, which illustrates both the accuracy and the numerical stability of the decaying wave method variants. Numerical results, including deflections at various points at various frequencies as well as mode shapes, are presented, and comparisons are offered. The numerical results demonstrate the accuracy and reliability of both variants of the decaying wave method, and this is because advantages of three methods are combined in each variant.

Nomenclature

B_l, B_r = left and right boundary of structure
b = frame separation, in. or m
i, j, k = arbitrary stations; cells near boundary or forcing
m, n = cell number; cell near output
Q_{ext} = external load vector
q = displacement vector
R_l, R_r = left and right reflection matrices
S = state vector
T = transfer matrix
T_l, T_r = left and right transmission matrices
t = time, s
W = wave matrix or wave transfer matrix
w = normal panel deflection, in. or m
X = eigenvector matrix
x = coordinate in frame direction
y = coordinate in stringer direction
Λ, λ, λ' = diagonal matrix containing larger, smaller, and all eigenvalues
μ = wave vector
ω = frequency of applied harmonic load

Superscripts

frc = wave vector caused by external forcing
inc, out = incoming, outgoing waves

Subscripts

l, r = left or right cell side, propagation direction, or boundary
n = cell number
nz = nonzero part of state vector
11, 12, 21, 22 = submatrix designators

Introduction

TYPICAL transport aircraft fuselages have a skin composed of thin plate panels supported by attached thin-walled beams of open cross section. A full fuselage skin structure is admittedly difficult to model, but much of the fuselage's dynamic behavior can be captured by a much simpler structure: a flat, periodic, single row, simply supported skin-stringer structure of finite length. This one row structure, seen in Fig. 1, is designed to emulate somewhat a long circumferential strip of the fuselage structure between two supporting circumferential beams, whose effects are somewhat simulated by a simple support boundary condition. The assumptions of a flat and periodic structure, while designed to make the calculation easier, are not completely unreasonable. Thus, the simpler structure should contain much of the same dynamic behavior as sections of fuselage skin would.

The single row simply supported skin-stringer structure has been analyzed by many different researchers using several different methods. Lin[1] found the dynamic behavior of this structure analytically, using the bending and torsional characteristics of the stringers. His analysis gives some important results, such as the existence and location of frequency filter bands in the infinite structure, but it does not provide a simple way to get complete response curves for the finite or infinite structure. Further, were the boundary conditions at the top or bottom of the structure to change, this type of analysis becomes extremely difficult. Thus, it became necessary to look at this problem using a numerical method.

The first choice of numerical method for many engineers is the finite element method, and finite element codes are commonplace throughout industry. With regard to skin-stringer structures, Mei[2] obtained the finite element matrices for a thin-walled open cross-sectional stringer, and he takes into account coupled bending and torsional vibrations that commonly occur in this type of beam. Bogner et al.[3] derived a panel element using Hermite cubic polynomials for displacement patterns, which ensure continuity of displacement and slope at the element edges. The combination of these element types has led to finite element analysis of skin-stringer struc-

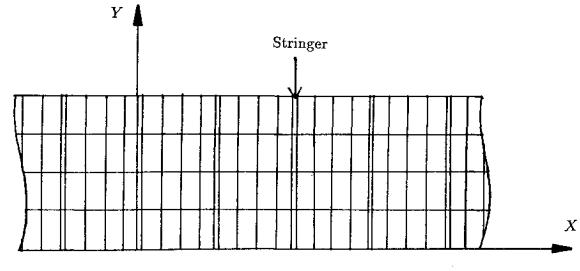

Fig. 1 One row skin-stringer structure illustrating discretization.

Received Sept. 16, 1991; revision received May 5, 1992; accepted for publication May 5, 1992.

*Graduate Research Assistant, Department of Aerospace Engineering and Engineering Mechanics, College of Engineering. Member AIAA.

†Associate Professor, Department of Aerospace Engineering and Engineering Mechanics, College of Engineering. Member AIAA.

tures, for free and forced vibration.[4-6] Unfortunately, a finite element method does not take into account the periodicity of the system, so it uses much more computation time and memory than other numerical methods. In addition, finite element methods work poorly when dealing with high-frequency excitation, and they contain a mild numerical instability.

To take advantage of the periodic and essentially one-dimensional nature of this structure, many researchers have used the transfer matrix method. The advantages of this method are that it requires modeling of only a periodic unit of the structure and that it eliminates intermediate nodal variables. Thus, the transfer matrix method uses much less computation time than a finite element method, while being easier to solve than a normal analytic method. The transfer matrix method was originally descended from methods developed by Holzer[7] and Mykelstad,[8] and it has been applied to several different one-dimensional problems.[9-14] Lin and Donaldson[15] provided a good overview of transfer matrix methods, and they concentrated on the application of transfer matrix methods to analysis of skin-stringer structures. Note that this structure, when modeled exactly, is multiple monocoupled, and the response curves for long structures at high frequencies can be obtained from transfer matrices by using work done by Igusa and Tang.[16] A different way of obtaining a transfer matrix, the finite element-transfer matrix analysis, was suggested by Dokanish[17] to get a solution technique with the advantages of both a finite element method and a transfer matrix method. McDaniel and Eversole[18] extended this idea to analyze the free vibration of a skin-stringer structure. Unfortunately, all transfer matrix methods suffer from acute numerical instability, and so they are not accurate either for long but finite structures or at high frequencies.

A method that retains the advantages of the transfer matrix method while possessing numerical stability is the decaying wave method. Yong and Lin[19,20] engineered this method for long but finite space truss structures, using an approach similar to von Flotow's.[21] Recently, Chen and Pierre[22] have used this method with an exact beam formulation to solve for the dynamics of space beam structures, while Huntington[23] used this method with a finite element formulation to analyze a single and multiple row damped skin-stringer structure with various boundary conditions. The decaying wave method is similar to standard wave propagation methods, in that it looks at traveling and damping disturbances propagating and reflecting through the structure. The decaying wave method is much faster than finite element codes because, like a transfer matrix method, it eliminates intermediate nodal variables. The decaying wave method also has the ease of modeling of a standard transfer matrix method, because it uses the transfer matrices in its formulation. More importantly, this method is completely free of the numerical instability that plagues the transfer matrix and finite element methods. However, the system studied must be at least lightly damped to ensure this stability. The decaying wave method is most effective when dealing with long periodic or piecewise periodic systems, and it takes rather more time and memory to solve structures that constantly change characteristics.

This work will obtain and examine the frequency response of a flat, single row, damped, periodic, simply supported skin-stringer structure using the decaying wave method. The initial modeling of a periodic unit will be done using both an exact method given by Lin and Donaldson[15] and a finite element method put forth by McDaniel and Eversole.[18] The results for a damped periodic structure of six bays will be compared to those obtained in Ref. 15 in the undamped case, and the results for a 500-bay damped structure will be compared to those obtained in Refs. 1 and 18 for an infinite, undamped, periodic structure. In addition, individual panel deflections will be found at the edges of frequency groups, and will be compared with mode shapes obtained in Ref. 1.

The original contributions of this work are as follows: 1) It introduces and tests the accuracy of the decaying wave method based on an exact formulation and based on a finite element formulation for this structure, combining the advantages of wave propagation techniques, transfer matrices, analytic methods, and finite element formulations. 2) It obtains accurate response curves for the long but finite, periodic, damped single row structure at moderate to high frequency.

Analytical Formulation

Overall, the decaying wave method is a variant of a transfer matrix method; indeed, knowledge of the transfer matrices in all periodic units in the structure is required, so the decaying wave method can be used only to analyze one-dimensional systems or multidimensional systems that can be formulated in a one-dimensional manner. In addition, the decaying wave method works only if the system has some structural damping; damping provides a simple way to determine a wave's direction of propagation, which, as will be shown subsequently, is of fundamental importance in establishing the numerical stability of the method.

Transfer matrix methods are now widely used, though not as widely as finite element methods. Their primary advantage is that they drastically reduce the number of unknowns in a structure by eliminating intermediate nodal variables, and the decaying wave method keeps this advantage. As previously mentioned, it is first necessary to obtain the transfer matrix for each type of periodic unit in the structure being considered. A transfer matrix shows the variation in the x direction of the mechanical state of the system, which is given by a state vector whose components represent all of the unknowns needed to completely describe the motion of the system at a certain station. Note that there are many choices of state vectors, and note further that different transfer matrix formulations will use drastically different state vectors.

To use transfer matrices to analyze a structure, the structure's forces and displacements must vary in one dimension only. If our structure is studied analytically, the displacement of the structure is assumed to be given by

$$w(x, y, t) = \sum_{k=1}^{n} e^{i\omega t} X_k(x) \sin \frac{k\pi y}{b} \tag{1}$$

where each $X_k(x)$ is a function of x alone; the problem becomes one dimensional. Lin and Donaldson[15] give a transfer matrix for each mode (e.g., each value of k) that shows how the displacement, slope, bending moment, and shear forces vary in the x direction. The equations of motion for a flat rectangular plate and a thin-walled beam are used to get the exact transfer matrix used in this article. For more details, see Ref. 15.

Similarly, McDaniel and Eversole[18] show how a finite element-transfer matrix method can reduce this problem to a one-dimensional form by formulating the state vector components as the forces and displacements at various y locations at a given x station. Because the state vector already takes into account the variation of forces and displacements in the y direction, the state vector will vary in the x direction only. Thus, the problem also becomes one-dimensional when formulated in this manner.

In addition, some words need to be said about the particular finite element formulation used in this study and in Ref. 18. This finite element formulation uses rectangular plate elements of the type developed by Bogner,[3] which approximates the element deflection with superpositions of Hermite polynomials in the x direction multiplied by similar polynomials in the y direction, to ensure that deflection and slope are continuous throughout the entire assembled finite element model. The beam elements used were developed by Mei[2] and include torsional warping effects. It should be mentioned that each stringer node has four degrees of freedom, whereas each panel node has only three; the stringer's extra degree of freedom comes from this warping. It is reasonable to assume at each stringer node that either no warping torsion is put on the beam

(as is assumed at all interior nodes) or the beam is not permitted to warp at that node (with some boundary conditions). These extra conditions are used to give the stringer three effective degrees of freedom at each node, so that it can be incorporated better with the plate elements, while accounting for this warping behavior common in these beams.

Standard assembly procedures are used to get the stiffness and mass matrices for a stringer or panel strip from the elemental mass and stiffness matrices. These assembled matrices are combined into a dynamic stiffness matrix for the strip or stringer, which is then made to satisfy boundary conditions. Matrix algebra transforms these dynamic stiffness matrices into transfer matrices; these transfer matrices for strip and stringer are combined to give a unit cell transfer matrix. Specific details about this formulation can be found in Ref. 23.

Once the transfer matrix across a periodic unit in the structure has been found, using either formulation, the next step is to determine the eigenvectors and eigenvalues of this transfer matrix; there are commercially available subroutines that can do this. Then these eigenvectors and eigenvalues are used to transform the state vector and transfer matrix into a wave vector and wave matrix, which, as will be seen, are easier to deal with for periodic structures. The state vectors across the nth unit cell in the structure are related by

$$\{S(n_r)\} = [T]_n \{S(n_l)\} \tag{2}$$

where $S(n_r)$ is a state vector on the right of cell n, $S(n_l)$ the state vector on the left of that same cell, and $[T]_n$ the transfer matrix across the nth cell.

By definition, eigenvectors and eigenvalues of a cell transfer matrix can be combined to give the following matrix equation:

$$[T]_n [X]_n = [X]_n [\lambda']_n \tag{3}$$

where $[X]_n$ is a matrix whose columns are the eigenvectors $\{X\}_i$ of the transfer matrix across the nth unit cell $[T]_n$, and $[\lambda']_n$ is a diagonal matrix containing the eigenvalues λ_i of that transfer matrix. Of course, the order of eigenvectors in $[X]_n$ should be the same as the order of the corresponding eigenvalues in $[\lambda']_n$. We now adopt a transformation, of the form

$$\{\mu(x)\} = [X]_n^{-1} \{S(x)\} \tag{4}$$

where $\mu(x)$ represents what will be called a wave vector. If Eq. (4) is rewritten slightly, it is evident that $\{S\} = \sum \mu_i \{X\}_i$, so that each component of the wave vector shows how much the corresponding eigenvector contributes to the total motion of the structure at that x station. In a periodic structure, the eigenvectors do not change from cell to cell, but the components of the wave vector do, so each eigenvector can be said to be a type of wave that propagates through the structure with an effective amplitude given by a component of the wave vector $\{\mu\}$. Note that a combination of Eqs. (2–4) shows how the wave vector transfers across the nth unit cell:

$$\{\mu(n_r)\} = [\lambda']_n \{\mu(n_l)\} \tag{5}$$

and thus the transfer matrix of the wave vector, or the wave matrix, across a unit cell is simply the diagonal eigenvalue matrix $[\lambda']$. Thus, some discussion about the eigenvalues of a transfer matrix is in order.

It is known that the eigenvalues of a transfer matrix always come in reciprocal pairs.[22] In general, the eigenvalues are complex, and they represent the change in both amplitude and phase for the components of the wave vector $\{\mu\}$ across a unit cell. A damped system will not have any pairs of eigenvalues with unit magnitude (which work out to be complex conjugates); therefore, half of the eigenvalues will have magnitudes less than one, and half will have magnitudes greater than one. The eigenvalues in a reciprocal pair represent the same "wave type" traveling in opposite directions; the eigenvalue whose magnitude is less than one represents that mode as traveling and decaying to the right, whereas the eigenvalue that has a magnitude larger than one represents that mode propagating to the left.

The eigenvalues will be reordered so that the smaller ones come in the first half of the matrix and the larger ones come in the second half; the most convenient way to do this is to place the eigenvalues in $[\lambda']$ in ascending order. Of course, the eigenvectors and wave vector components must be reordered similarly. This reordering will effectively separate the right-traveling waves from the left traveling, which will allow wave propagation techniques to be used. The reordering of the eigenvalues will give a new wave matrix across the nth unit cell $[W(n_l, n_r)]$:

$$[W(n_l, n_r)] = \begin{bmatrix} \lambda & 0 \\ 0 & \Lambda \end{bmatrix} \tag{6}$$

It is possible to reorder in such a way that $\Lambda = \lambda^{-1}$, but this is not necessary, and it will not occur if the eigenvalues are put in order of ascending magnitude. Also, from Eq. (4) and the condition of state vector continuity, the wave matrix at an interface between the right side of cell n and the left side of cell $n + 1$ is given by

$$[W(n_r, n+1_l)] = [X]_{n+1}^{-1} [X]_n \tag{7}$$

Note that while the state vector will be continuous at the interface of two different cell types (with different eigenvector matrices), the wave vector will not. However, both the state vector and the wave vector are continuous across similar cells, so a wave matrix across a periodic group of cells from m to n can easily be obtained from Eqs. (6) and (7), resulting in

$$[W(m_l, n_r)] = \begin{bmatrix} \lambda^{(n-m+1)} & 0 \\ 0 & \Lambda^{(n-m+1)} \end{bmatrix} \tag{8}$$

Equation (8) shows that, to get the wave matrix for a group of identical cells, it is only necessary to take eigenvalues to powers, instead of doing many matrix multiplications; this will give the decaying wave method a speed and accuracy advantage over a standard transfer matrix method for long periodic structures. Note that Eq. (8) also shows that the eigenvalues in λ, with magnitudes less than one, will give diagonal elements in the group wave matrix that will be much less than one, whereas the eigenvalues in Λ will give diagonal elements that will become much larger than unity.

It is this latter group that causes all the trouble in a transfer matrix method, since over a long structure certain components of the wave vector will become very large indeed but must "cancel out" somewhat to satisfy the condition, whatever it may be, on the right boundary, which leads to gross roundoff error and related numerical problems. In essence, the transfer matrix method follows some disturbances in the direction in which they appear to grow, which leads to numerical disaster for long structures or high frequencies. The decaying wave method, on the other hand, will follow all disturbances in the directions in which they damp, and is, therefore, always numerically stable, because there are no growing disturbances and, hence, no growing errors. To do this, the decaying wave method will change the problem formulation from wave matrices to transmission and reflection matrices.

Consider Fig. 2, which is a representation of a group of cells (similar or dissimilar) from station i to station j, where $i < j$, and the wave vectors on either end. It is clear from the figure that $\{\mu_r(i)\}$, the right traveling disturbances at the left of this cell group, and $\{\mu_l(j)\}$, the disturbances at the right end of the cell group which travel left, are incoming waves; $\{\mu_l(i)\}$ and $\{\mu_r(j)\}$ are outgoing waves. It is clear that, within the confines of this cell group, $\{\mu_r(i)\}$ and $\{\mu_l(j)\}$ do not affect each other. Further, the outgoing waves are superpositions of

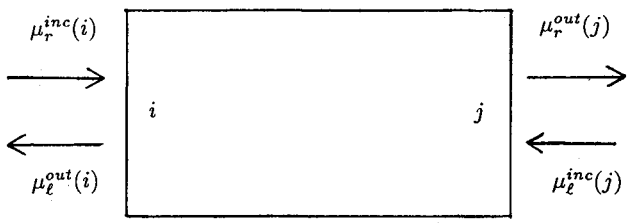

Fig. 2 Incoming and outgoing disturbances on either end of a typical cell group in terms of wave vectors.

the effects of the right- and left-incoming waves, so it is possible to formulate the problem with only left-incoming or right-incoming waves, then superpose the effects of each to get the total outgoing waves.

The relation between the wave vectors across the cell group (i, j) is given by[20]

$$\begin{Bmatrix} \mu_r^{\text{out}}(j) \\ \mu_l^{\text{inc}}(j) \end{Bmatrix} = \begin{bmatrix} W_{11}(i,j) & W_{12}(i,j) \\ W_{21}(i,j) & W_{22}(i,j) \end{bmatrix} \begin{Bmatrix} \mu_r^{\text{inc}}(i) \\ \mu_l^{\text{out}}(i) \end{Bmatrix} \tag{9}$$

Suppose now that we wish to find the left transmission matrix $[T_l(i, j)]$. If the right incoming wave components are set to zero, the left transmission matrix can be found by obtaining the matrix relation between the left outgoing wave and the left incoming wave:

$$\{\mu_l^{\text{out}}(i)\} = [T_l(i, j)]\{\mu_l^{\text{inc}}(j)\} \tag{10}$$

The matrix relation between the right outgoing wave and the left incoming wave will similarly yield the left reflection matrix, denoted by $[R_l(i, j)]$. Matrices which show how a right traveling wave transmits and reflects through this cell group, $[T_r(i, j)]$ and $[R_r(i, j)]$, can be found in the same manner. This results in the following expressions for the transmission and reflection matrices[20]:

$$\begin{aligned} [R_r(i,j)] &= -[W_{22}(i,j)]^{-1}[W_{21}(i,j)] \\ [T_r(i,j)] &= [W_{11}(i,j)] - [W_{12}(i,j)][W_{22}(i,j)]^{-1}[W_{21}(i,j)] \\ [R_l(i,j)] &= [W_{12}(i,j)][W_{22}(i,j)]^{-1} \\ [T_l(i,j)] &= [W_{22}(i,j)]^{-1} \end{aligned} \tag{11}$$

where $[W_{m,n}]$ are the submatrices of the wave matrix, shown in Eq. (9).

Just as the reflection and transmission matrices can be formed from the wave matrix, the wave matrix can be written in terms of reflection and transmission matrices:

$$[W(i,j)] = \begin{bmatrix} T_r - R_l T_l^{-1} R_r & R_l T_l^{-1} \\ -T_l^{-1} R_r & T_l^{-1} \end{bmatrix} \tag{12}$$

where the cell group designation (i, j) is assumed for the reflection and transmission matrices. The wave matrix is a type of transfer matrix, and so, if the wave matrices in two adjacent regions are known, they can be multiplied to get a transfer matrix over the entire region:

$$[W(i,k)] = [W(j,k)][W(i,j)] \tag{13}$$

If the wave matrices in Eq. (13) are written as in Eq. (12) and then multiplied, and finally Eq. (11) are applied, the combined transmission and reflection matrices over (i, k) can be found in terms of those over group (i, j) and group (j, k):

$$\begin{aligned} R_r(i,k) &= R_r(i,j) + T_l(i,j)R_r(j,k)[I - R_l(i,j)R_r(j,k)]^{-1}T_r(i,j) \\ T_r(i,k) &= T_r(j,k)[I - R_l(i,j)R_r(j,k)]^{-1}T_r(i,j) \\ R_l(i,k) &= R_l(j,k) + T_r(j,k)R_l(i,j)[I - R_r(j,k)R_l(i,j)]^{-1}T_l(j,k) \\ T_l(i,k) &= T_l(i,j)[I - R_r(j,k)R_l(i,j)]^{-1}T_l(j,k) \end{aligned} \tag{14}$$

The numerical stability of the decaying wave method can now be addressed. First, the transmission and reflection matrices over a group of identical cells are found by a combination of Eqs. (8) and (11):

$$\begin{aligned} [R_l(m_l, n_r)] &= [R_r(m_l, n_r)] = [0] \\ [T_r(m_l, n_r)] &= [\lambda^{(n-m+1)}] \\ [T_l(m_l, n_r)] &= [\Lambda^{-(n-m+1)}] \end{aligned} \tag{15}$$

The zero values for the reflection matrices in Eqs. (15) are expected, since there is no reflection within a group of identical cells. Note that both transmission matrices have every element less than one, because disturbances decay as they travel through the structure; the transmission matrices follow disturbances in the directions in which they damp. Now if there is a new cell type at $n + 1$, then the combined reflection and transmission matrices become[20]

$$\begin{aligned} [R_l(m_l, n+1_l)] &= [R_l(n_r, n+1_l)] \\ [R_r(m_l, n+1_l)] &= [\Lambda]^{-(n-m+1)}[R_r(n_r, n+1_l)][\lambda]^{(n-m+1)} \\ [T_r(m_l, n+1_l)] &= [T_r(n_r, n+1_l)][\lambda^{(n-m+1)}] \\ [T_l(m_l, n+1_l)] &= [\Lambda^{-(n-m+1)}][T_l(n_r, n+1_l)] \end{aligned} \tag{16}$$

For example, note the expression for the right reflection matrix $[R_r]$. It shows clearly that the only right reflecting waves are those that travel through the cell group to the interface, reflect off of it, and travel back to the beginning of the cell group. It is evident that these reflection and transmission matrices follow all disturbances in the directions in which they travel and damp, and this leads to the decaying wave method's numerical stability.

The simple support boundary condition at the top and bottom of the structure was incorporated into the transfer matrix formulation earlier. Fortunately, the boundary conditions at the left and right ends of the structure are handled eloquently by the decaying wave method. The boundary conditions considered here, which are free, clamped, and simply supported, will require that exactly half of the elements in the state vector be zero. For example, suppose that there is a boundary on the left of cell i. Equation (4) can be reordered, and, when the requisite elements in the state vector are set to zero, the resulting expression at that boundary B_l is given by

$$\begin{Bmatrix} S_{nz}(B_l) \\ 0 \end{Bmatrix} = \begin{bmatrix} X'_{11}(i) & X'_{12}(i) \\ X'_{21}(i) & X'_{22}(i) \end{bmatrix} \begin{Bmatrix} \mu_r^{\text{out}}(B_l) \\ \mu_l^{\text{inc}}(B_l) \end{Bmatrix} \tag{17}$$

where the primes on the eigenvector submatrices are to denote the reordering. For example, were the boundary conditions at the left and right to be simple supports, all displacements and rotations about the x axis would be set to zero, as would all moments about the y axis; all other displacements and forces would be in S_{nz}. From this, it follows that a reflection matrix for the left boundary can be written as

$$[R_l(B_l, i_l)] = -[X'_{21}(i)]^{-1}[X'_{22}(i)] \tag{18}$$

A similar procedure employed for the right boundary B_r, just to the right of cell j, gives the reflection matrix for that boundary:

$$[R_l(j_r, B_r)] = -[X'_{22}(j)]^{-1}[X'_{21}(j)] \tag{19}$$

Other types of boundary conditions, such as an attached spring or mass, will put half of the state vector components in terms of the other half; the procedure will be more complicated, but it is possible to model even these boundary conditions with a reflection matrix. Of course, it does not make sense to speak of transmission matrices at a boundary, and these are assumed to be zero.

The next step in the formulation is to generate reflection matrices from the forcing station to both boundaries by using the combination procedure as many times as necessary, including the boundary reflection matrices themselves. Then the state vectors on either side of the forcing station are written in terms of the outgoing and reflected wave subvectors, using Eq. (4). Note that the reflected wave subvector is the combined reflection matrix multiplied by the outgoing wave subvector for that side of the structure. Finally, the state vectors are related to each other by continuity and force balance considerations. This leads to an expression that gives the outgoing waves to the right and left of the forcing station at the interface between cells k and $k+1$[20]:

$$\begin{Bmatrix} \mu_r^{\text{frc}}(k+1_l) \\ \mu_l^{\text{frc}}(k_r) \end{Bmatrix} = \begin{bmatrix} A_{11} & A_{12} \\ A_{21} & A_{22} \end{bmatrix}^{-1} \begin{Bmatrix} 0 \\ Q_{\text{ext}} \end{Bmatrix} \tag{20}$$

where

$$\begin{aligned} A_{11} &= X_{11}(k+1) + X_{12}(k+1)R_r(k+1_l, B_r) \\ A_{12} &= -X_{11}(k)R_l(B_l, k_r) - X_{12}(k) \\ A_{21} &= X_{21}(k+1) + X_{22}(k+1)R_r(k+1_l, B_r) \\ A_{22} &= -X_{21}(k)R_l(B_l, k_r) - X_{22}(k) \end{aligned} \tag{21}$$

Finally, wave propagation considerations allow the wave vector at the output station to be found. For example, suppose that the output station n_l is to the right of the forcing station k_l and, of course, the output station is to the left of the right boundary B_r. From wave propagation, the wave subvectors at the output station are related as follows:

$$\begin{aligned} \{\mu_l(n_l)\} &= [R_l(n_l, B_r)]\{\mu_r(n_l)\} \\ \{\mu_r(n_l)\} &= [T_r(k_l, n_l)\{\mu_r^{\text{frc}}(k_l)\} + [R_l(k_l, n_l)\{\mu_l(n_l)\} \end{aligned} \tag{22}$$

Equations (22) state that the right traveling waves at the output station eventually reflect off the right boundary (or somewhere before) and return as left traveling waves, and they also show that the right traveling waves are caused by transmission of the forced waves and possible additional reflection of the left traveling waves. Reflections on the other side of the forcing station are of no concern here, as they have already been taken into account when establishing the forced waves. From Eqs. (22) and (4), the displacement vector at the forced station can be found by:

$$\begin{aligned} q(n_l) = [X_{11}(n) + X_{12}(n)R_r(n_l, B_r)] \\ \times [I - R_l(k+1_l, n_l)R_r(n_l, B_r)]^{-1}T_r(k+1_l, n_l)\mu_r^{\text{frc}} \\ (k+1<n) \end{aligned} \tag{23}$$

A similar argument can be applied to find the displacement at station m_r, where $m<k$:

$$\begin{aligned} q(m_r) = [X_{11}(m) + R_l(B_l, m_r) + X_{12}(m)] \\ \times [I - R_r(m_r, k_r)R_l(B_l, m_r)]^{-1}T_l(m_r, k_r)\mu_l^{\text{frc}} \ (m<k) \end{aligned} \tag{24}$$

Overall, the transfer matrices themselves have no special significance in the decaying wave method. Their eigenvectors and eigenvalues are used to transform the problem into wave vectors and wave matrices. These wave matrices are also of no importance, except to obtain the reflection and transmission matrices. The significant steps in the analysis—the combination procedure, boundary conditions, external forcing, and the final output—were all put into terms of the eigenvector matrices (or submatrices) and the transmission and reflection matrices alone. This ensures numerical stability in the crucial parts of the calculation, and it allows the decaying wave method to analyze long but finite systems, even at high frequency, which is the regime that creates problems for both the transfer matrix method and the finite element method.

Results and Discussion

A single row simply supported skin-stringer structure, similar to that in Fig. 1, was analyzed. Numerical results were obtained using two different formulations of the decaying wave method, one based off of an exact solution transfer matrix and the other founded in a finite element formulation. Comparisons were made to validate the proposed method's accuracy and stability. All relevant structural data for the panels and stringers used in this article are listed in Table 1; these data were originally obtained by Lin[1] from Boeing Aircraft Co. and were used to generate the results found in Refs. 1, 15, and 18, which are used for comparison purposes. Note that this article analyzes a lightly damped structure,

Table 1 List of physical properties for panels and stringers

Characteristic	Symbol	English units	Metric units
General			
Young's modulus	E	10.5×10^6 lb/in.^{2}	7.2391×10^{10} N/m^2
Poisson's ratio	ν	0.3	0.3
Density	ρ	2.6166×10^{-4} lb s^2/in.^{4}	2796 kg/m^3
Structural damping	γ	0.01	0.01
Panel			
Thickness	h	0.04 in.	1.016×10^{-3} m
Frame separation	b	20.0 in.	0.5080 m
Stringer separation	a	8.20 in.	0.2083 m
Stringer			
X-section area	A	0.2302 in.^{2}	1.485×10^{-4} m^2
Warping constant	C_{ws}	0.01649 in.^{6}	4.428×10^{-12} m^6
St. Venant constant	C	2.263×10^{-4} in.^{4}	9.419×10^{-11} m^4
Polar moment of inertia	I_s	0.254 in.^{4}	1.057×10^{-7} m^4
Centroidal bending inertia	I_η	0.122 in.^{4}	5.078×10^{-8} m^4
Centroidal prod of inertia	$I_{\eta\zeta}$	0	0
Horizontal location of S	S_x	0	0
Vertical location of S	S_z	0.082 in.	2.083×10^{-3} m
Horizontal location of C	C_x	0	0
Vertical location of C	C_z	0.802 in.	2.037×10^{-2} m

whereas the results used for comparison in the references are for an undamped structure; it will be seen that the damping does not affect the results appreciably. To test the accuracy of the finite element-decaying wave (FEDW) method and the exact solution-decaying wave (ESDW) method, two structures will be analyzed, differing only in length. The first structure is six bays long, has stringers on both ends, has a free boundary condition on the left and right ends, and is simply supported at the top and bottom; Lin and Donaldson[15] found the first 12 natural frequencies for this structure, against which the response peak frequencies for both the FEDW and ESDW methods will be compared. The second structure analyzed is 500 bays long and also has free boundary conditions, and both decaying wave methods will be used to find frequency band ranges, which will be compared against those ranges in an infinite, undamped structure found analytically in Ref. 1 and found using a finite element-transfer matrix scheme in Ref. 18. Also, in the 500-bay case, the deflection of a single panel, obtained at frequencies near the frequency band edges, will be compared with mode shapes found in Ref. 1 for the infinite case.

It has long been known that periodic structures have natural frequencies that fall into certain frequency groups, which means that the first several natural frequencies will fall close together, then the next several frequencies will be close to each other but not to the first several, and so on. Further, for many types of periodic structure, including this one, the number of frequencies in each group is equal to the number of periodic units in the structure. Thus, for a six-bay structure, the response curves ought to have six peaks in each frequency group. This is illustrated nicely in the response curves (obtained by both methods) for the structure's first and second frequency group, which are Figs. 3 and 4, respectively. However, Fig. 4 is somewhat misleading; it turns out that the third frequency group begins immediately after the second group, and the peak at 315 Hz actually belongs to this third group. To see the six peaks in the second group more clearly, refer to the ESDW response curve in Fig. 5, in which the damping factor

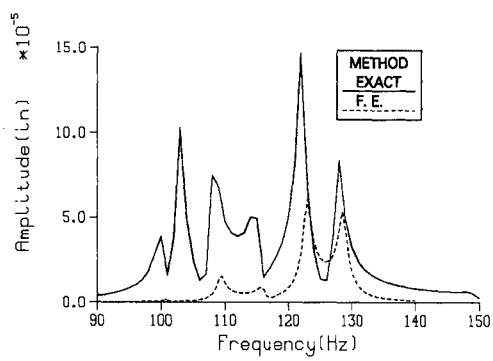

Fig. 3 First frequency group of the six-bay case obtained by exact solution and finite element variant.

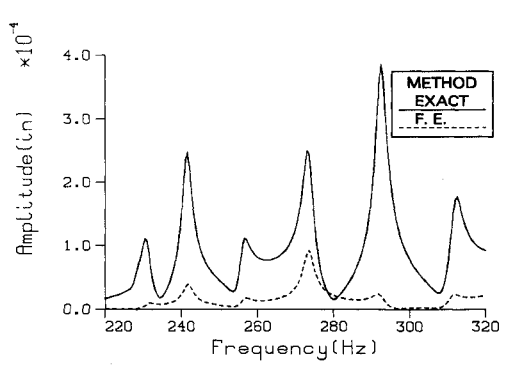

Fig. 4 Second frequency group of the six-bay case obtained by exact solution and finite element variant.

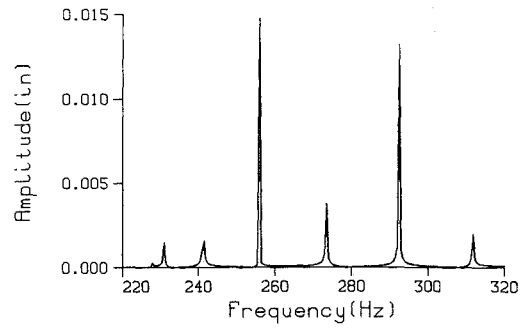

Fig. 5 Second frequency group of the six-bay case obtained by exact solution variant with extremely low damping to find the first two peaks.

Table 2 Comparison of peak frequencies in six-bay case found by decaying wave (DW) variants with those obtained in Ref. 15

Peak	Exact	FE[a]	TM[b](Ref. 15)
1	100.0	101.0	100.2
2	103.0	104.0	103.4
3	108.5	109.5	108.7
4	114.5	115.5	115.4
5	122.0	123.0	122.6
6	128.0	128.5	128.5
7	228.0	229.5	228.5
8	231.0	232.0	231.7
9	241.5	241.5	243.0
10	256.0	257.0	257.5
11	273.5	273.5	274.7
12	292.5	291.5	295.0

[a]Finite element. [b]Transfer matrix.

has been reduced from 0.01 to 1×10^{-8} to reduce peak interference; note that there are two peaks very close together near 230 Hz. Thus, the second frequency group ends at approximately 300 Hz.

Note that the individual peak heights in the FEDW results are quite different than the ESDW results, as shown in Figs. 3 and 4. This difference is primarily caused by the necessity of using different forcing functions in each method. In the FEDW method, loads can only be applied to the nodes, so a point load was applied at node six (three-fourths of the way down the eight-element structure), and the output, at the output station, was also taken at node six. But for the ESDW method, it was required to apply forces that vary sinusoidally in the vertical direction, even though the output could be taken at the same place. Therefore, it is expected that the peak heights should change somewhat between the two sets of results. However, note that the peak frequencies are extremely close between the two sets of results. This is best illustrated in Table 2, where the peak frequencies for both sets of results are compared to each other and to those in the last column obtained from Ref. 15 with an exact solution transfer matrix. All of these frequencies, which were obtained by different methods, compare very well to each other.

Response curves for a long, finite structure (500 bays, in this case) are difficult to obtain by a transfer matrix method, for reasons of numerical instability. An analytic method is extremely difficult to set up for this problem; a finite element method would take a large amount of computation time and memory, and, using it, one would also suffer some numerical problems while analyzing this structure. A decaying wave method, on the other hand, can analyze this structure with virtually no trouble at all. We do not expect that a typical structure will in fact extend some 342 ft in length, but, if the decaying wave methods are accurate over a structure that is this long, they will produce good results for any shorter structure as well. The 500-bay case will, therefore, illustrate the numerical stability inherent in the decaying wave methods.

This case was also chosen for study because its characteristics are similar to that of an infinite, undamped structure, which has been studied by many researchers.

In the six-bay case, it made sense to talk of frequency groups, because it was easy to denote and count the individual peaks. The 500-bay case is a different matter, because the 500 peaks present in each group crowd together and merge into a smooth response curve; for long structures, the frequency groups become analogous to frequency passbands. In an undamped infinite structure, where the frequency groups have completely transformed into frequency bands, Ref. 1 shows that the edges of these bands occur at certain distinct frequencies, where every panel in the structure vibrates either exactly in phase or exactly out of phase with its neighbors and where the stringers deflect in either pure twisting or pure bending. These criteria give four transcendental equations in frequency, the solutions to which are the edges of the frequency bands in the undamped infinite structure.

The response curves in the first few passbands found by the ESDW method and the FEDW method are shown in Figs. 6 and 7. To obtain these response curves, a periodic point load of 1 lb was applied at a station one-half of the length of the structure, at three-fourths the width; output was taken at a station one-third of the way along the structure, at three-fourths the width. Although an undamped structure has frequency passbands with distinct beginning and ending frequencies, the response curves obtained here for the damped structure begin and end smoothly and do not have distinct edges. Thus, it is necessary to estimate the frequencies of the band edges by setting an arbitrary threshold amplitude for each edge, usually one-thousandth of the peak amplitude for that group, and finding the frequency corresponding to that amplitude. These estimations are compared in Table 3 to the solutions of the transcendental equations mentioned previously. Note that the frequency band edges that are actually

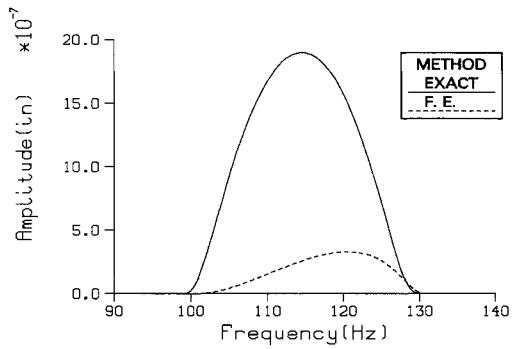

Fig. 6 First frequency group of the 500-bay case obtained by exact solution and finite element variant.

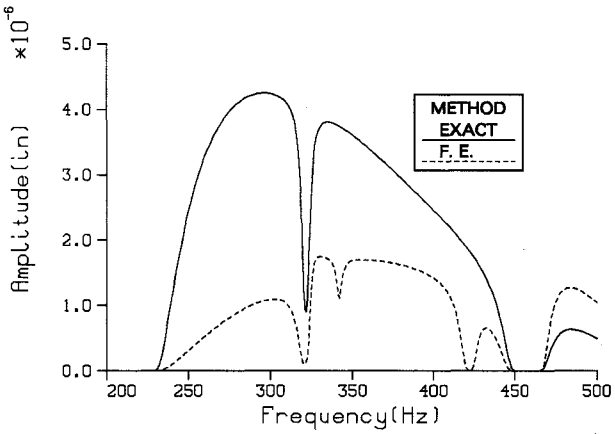

Fig. 7 Second, third, and fourth frequency groups of the 500-bay case obtained by exact solution and finite element variant.

Table 3 Comparison of frequency band edges in 500-bay case found by DW variants with those obtained in Refs. 1 and 18[a]

Band edge	ESDW	FEDW	Analytic[1]	FETM[18]
Beg 1	99	100	98.846	99.101
End 1	130	131	130.175	126.655
Beg 2	230	231	228.800	219.383
End 2	321	321	(319.763)	350.146
Beg 3	323	323	323.255	
End 3	449	449	(448.777)	

[a]Results in parentheses denote solutions to equations from Ref. 1 that are not listed in that reference.

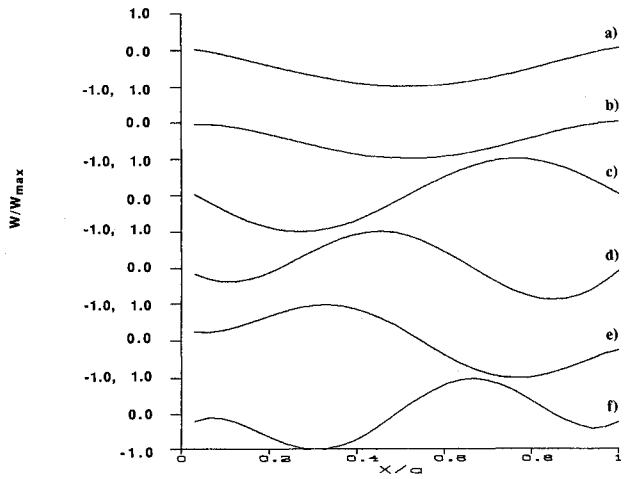

Fig. 8 Mode shapes obtained at various frequencies for the 500-bay case using finite element variant: a) 100 Hz; b) 130 Hz; c) 231 Hz; d) 319 Hz; e) 323 Hz; f) 449 Hz. There are stringers at 0 and 1.

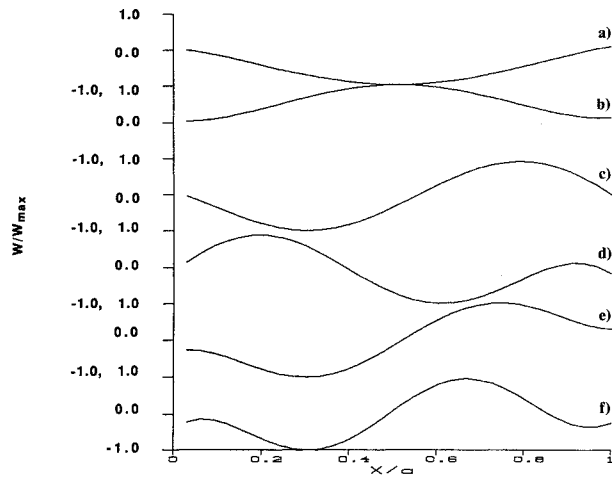

Fig. 9 Mode shapes obtained at various frequencies for the 500-bay case using exact solution variant: a) 100 Hz; b) 131 Hz; c) 230 Hz; d) 319 Hz; e) 325 Hz; f) 450 Hz. There are stringers at 0 and 1.

listed in Ref. 1 are slightly incorrect, because there is a second solution to one equation (in this case, at 319.763 Hz) before the first solution to another equation (at 323.255 Hz), and this was not taken into account; these frequencies are close together, and away from 320 Hz, the root at 323.255 Hz dominates the system behavior. Note that both the ESDW results and the FEDW results agree quite well with Lin's band edges. There appear to be more bands in the FEDW results from 200 to 450 Hz than there should be because the FEDW modeling is not exact and introduces some minor but unavoidable numerical problems when the cell transfer matrix is formed. However, even with these problems, the FEDW response curves are remarkably similar to the ESDW results, and the

Table 4 Comparison of criteria of mode shapes (stringer bending or twisting; in or out of phase with neighboring panels) found using DW variants with those criteria of mode shapes found in Ref. 1

Band edge	Analytic[1]	ESDW	FEDW
Beg 1	Tw[a] Out	Tw Out	Tw Out
End 1	Be[b] In	Be In	Be In
Beg 2	Tw In	Tw In	Tw In
End 2	Tw Out	Tw Out	Tw In
Beg 3	Be Out	Be Out	Be Out
End 3	Tw In	Tw In	Tw In

[a]Twisting. [b]Bending.

FEDW method has good accuracy when dealing with this problem.

To further illustrate the accuracy of the decaying wave methods, and to better locate the band edges in the FEDW results, it was decided to obtain the deflections of a typical panel at the frequency band edges and compare these with the mode shapes from Ref. 1 at these edges. These panel deflections were found by first getting the complete state vector at the output station and finding the relevant deflection. Transfer matrices were found over a small fraction of a bay, and these were multiplied by the state vector repeatedly to obtain the state vector at many stations within the panel. The relevant deflections within the panel were taken from these state vectors and plotted versus location on the panel. Panel deflections at each edge frequency obtained by the FEDW method and the ESDW method are shown in Figs. 8 and 9, respectively. A qualitative comparison of the mode shapes in figures 8 and 9 with those found by Lin[1] is found in Table 4. For purposes of comparison, mode shapes are defined by the type of stringer deflection (bending or twisting) and by whether neighboring stringers vibrate in or out of phase. It is evident from Table 4 that the panel deflections obtained from this analysis are identical to the mode shapes presented in Ref. 1, supporting the edge frequency results.

Conclusions

Two formulations of the decaying wave method were employed to accurately obtain response curves for a lightly damped periodic single row skin-stringer structure with simple support boundary conditions. An exact solution transfer matrix and a finite element transfer matrix approach were used to formulate the decaying wave method, which, therefore, combined the advantages of wave propagation methods, transfer matrices, finite element formulations, and analytic solutions. Results were obtained using each method. The exact solution decaying wave results compared very well with previous results, showing the accuracy and stability of the decaying wave method in general on both short and long structures. Further, actual response curves were found using the ESDW method for a very long but finite structure, which verify and extend previous results[1] for an infinite structure.

Overall, the finite element decaying wave results also compared very well with published results. The FEDW response curves illustrated the same crucial characteristics found in the ESDW results. Most discrepancies between the two sets of results are believed to be caused by different forcing functions. There are some minor but unavoidable problems with the finite element modeling itself that affect the response curve in the third frequency passband, but even these problems generate only minor discrepancies in the results.

The method of choice for this particular structure is the ESDW method, which combines numerical stability with a precise solution over both a short and a long structure while taking up relatively little computation time and memory. However, were the boundary conditions at the top and bottom of the structure to change, or were one to investigate a structure of multiple rows, the exact solution transfer matrix is no longer valid; thus, the ESDW method becomes impossible. On the other hand, the barely less accurate but far more flexible FEDW method can be used to analyze these problems, and, as the method has been found to be very accurate over the simpler structure, the results obtained by the FEDW method over a more complicated structure would be accurate as well. Thus, a finite element transfer matrix decaying wave method can be employed without trepidation to solve any complicated periodic skin-stringer type structure more accurately and efficiently than any of the involved methods used individually.

Acknowledgments

This work was supported by National Science Foundation Grant MSM-9008953. Furthermore, special thanks go to Eliezer Lubliner, who wrote some of the subroutines of the Fortran code used to obtain the results.

References

[1]Lin, Y. K., "Free Vibration of Continuous Skin-Stringer Panels," *Journal of Applied Mechanics,* Vol. 27, Dec. 1960, pp. 669–676.

[2]Mei, C., "Coupled Vibrations of Thin-Walled Beams of Open Section Using the Finite Element Method," *International Journal of the Mechanical Sciences,* Vol. 12, April 1970, pp. 883–891.

[3]Bogner, F. K., Fox, R. L., and Schmidt, L. A., "Generation of Inter-Element Compatible Stiffness and Mass Matrices by the Use of Interpolation Formulas," *Proceedings of the First Conference on Matrix Methods in Structural Mechanics,* Defense Documentation Center, Arlington, VA, 1966.

[4]Lindberg, G. M., and Olsen, M. D., "Vibration Modes and Random Response of Multi-Bay Panel Systems Using Finite Elements," National Research Council of Canada, Ottawa, Canada, LR-492, 1967.

[5]Lindberg, G. M., Olsen, M. D., and Westly, R., "The NAE Acoustic Test Facility—Structural Response to Random Noise," *Quarterly Bulletin of the Division of Mechanical Engineering and the Aeronautical Establishment,* National Research Council of Canada, Ottawa, Canada, 1967.

[6]Yurkovich, R. A., Schmidt, J. H., and Zak, A. R., "Dynamic Analysis of Stiffened Panel Structures," *Journal of Aircraft,* Vol. 8, No. 3, 1971, pp. 149–155.

[7]Holzer, H., *Die Berechnung der Drehschwingungen* [Calculation of Rotary Oscillations], Springer-Verlag, Berlin, 1921.

[8]Mykelstad, N. O., "A New Method of Calculating Natural Modes of Uncoupled Bending Vibrations of Airplane Wings and Other Types of Beams," *Journal of Aeronautical Science,* April 1944.

[9]Pestel, E. C., and Leckie, F. A., *Matrix Methods in Elastomechanics,* McGraw-Hill, New York, 1963, Chaps. 3–7.

[10]Leckie, F. A., "The Application of Transfer Matrices to Plate Vibrations," *Ingenieur-Archiv,* Vol. 32, 1963, pp. 100–111.

[11]Lin, Y. K., McDaniel, T. J., Donaldson, B. K., Vail, C. F., and Dwyer, W. J., *Free Vibration of Continuous Skin-Stringer Panels with Non-Uniform Spacing and Panel Thickness, Part I,* Air Force Materials Lab., AFML-TR-64-347, Wright-Patterson AFB, OH, 1965.

[12]Vaicaitis, R., and Slazak, M., "Noise Transmission Through Stiffened Panels," *Journal of Sound and Vibration,* Vol. 70, March 1980, pp. 413–426.

[13]Chang, M. T., and Vaicaitis, R., "Noise Transmission into Semicylindrical Enclosures Through Stiffened Curved Panels," *Journal of Sound and Vibration,* Vol. 85, Jan. 1982, pp. 71–83.

[14]Lyrintzis, C. S., and Bofilios, D. A., "Moisture Effect on the Response of Orthotropic Stiffened Panel Structures," *AIAA Journal,* Vol. 28, No. 12, 1990, pp. 2117–2124.

[15]Lin, Y. K., and Donaldson, B. K., "A Brief Survey of Transfer Matrix Techniques with Special Reference to the Analysis of Aircraft Panels," *Journal of Sound and Vibration,* Vol. 10, Jan. 1969, pp. 103–143.

[16]Igusa, T., and Tang, Y., "Mobilities of Periodic Structures in Terms of Asymptotic Modal Properties," AIAA Paper 91-0945, April 1991.

[17]Dokanish, M. A., "A New Approach for Plate Vibrations: Combination of Transfer Matrix and Finite-Element Technique," Transactions of the ASME, Series B, *Journal of Engineering for Industry,* Vol. 94, May 1972, pp. 526–530.

[18]McDaniel, T. J., and Eversole, K. B., "A Combined Finite Element-Transfer Matrix Structural Analysis Method," *Journal of Sound and Vibration,* Vol. 51, Feb. 1977, pp. 157–169.

[19]Yong, Y., and Lin, Y. K., "Wave Propagation in Truss-Type Structural Networks," AIAA Paper 90-1082, April 1990.

[20]Yong, Y., and Lin, Y. K., *Propagation of Decaying Waves in Periodic and Piece-Wise Periodic Structures of Finite Length,* Center for Applied Stochastics Research, Boca Raton, FL, CAS 88-3, April 1988.

[21]von Flotow, A. H., "Disturbance Propagation in Structural Networks," *Journal of Sound and Vibration,* Vol. 106, March 1986, pp. 433–450.

[22]Chen, W. J., and Pierre, C., *Exact Linear Dynamics of Periodic and Disordered Truss Beams: Localization of Normal Modes and Harmonic Waves,* Univ. of Michigan, Ann Arbor, MI, 1991, pp. 1–21.

[23]Huntington, D. E., "Response Analysis of a Damped Skin-Stringer Structure Using a Modified Wave Propagation Method," M.S. Thesis, Department of Aerospace Engineering and Engineering Mechanics, San Diego State Univ., San Diego, CA, 1991.